Automated beam placement for breast radiotherapy using a support vector machine based algorithm

Xuan Zhao and Dewen Kong
Department of Electrical and Computer Engineering, Polytechnic Institute of New York University, Brooklyn, New York 11201

Gabor Jozsef and Jenghwa Chang
Department of Radiation Oncology, School of Medicine, Langone Medical Center, New York University, New York, New York 10016

Edward K. Wong
Department of Computer Science and Engineering, Polytechnic Institute of New York University, Brooklyn, New York 11201

Silvia C. Formenti
Department of Radiation Oncology, School of Medicine, Langone Medical Center, New York University, New York, New York 10016

Yao Wang[a)]
Department of Electrical and Computer Engineering, Polytechnic Institute of New York University, Brooklyn, New York 11201

(Received 2 March 2011; revised 16 March 2012; accepted for publication 19 March 2012; published 16 April 2012)

Purpose: To develop an automated beam placement technique for whole breast radiotherapy using tangential beams. We seek to find optimal parameters for tangential beams to cover the whole ipsilateral breast (WB) and minimize the dose to the organs at risk (OARs).
Methods: A support vector machine (SVM) based method is proposed to determine the optimal posterior plane of the tangential beams. Relative significances of including/avoiding the volumes of interests are incorporated into the cost function of the SVM. After finding the optimal 3-D plane that separates the whole breast (WB) and the included clinical target volumes (CTVs) from the OARs, the gantry angle, collimator angle, and posterior jaw size of the tangential beams are derived from the separating plane equation. Dosimetric measures of the treatment plans determined by the automated method are compared with those obtained by applying manual beam placement by the physicians. The method can be further extended to use multileaf collimator (MLC) blocking by optimizing posterior MLC positions.
Results: The plans for 36 patients (23 prone- and 13 supine-treated) with left breast cancer were analyzed. Our algorithm reduced the volume of the heart that receives >500 cGy dose (V5) from 2.7 to 1.7 cm^3 ($p = 0.058$) on average and the volume of the ipsilateral lung that receives >1000 cGy dose (V10) from 55.2 to 40.7 cm^3 ($p = 0.0013$). The dose coverage as measured by volume receiving >95% of the prescription dose (V95%) of the WB without a 5 mm superficial layer decreases by only 0.74% ($p = 0.0002$) and the V95% for the tumor bed with 1.5 cm margin remains unchanged.
Conclusions: This study has demonstrated the feasibility of using a SVM-based algorithm to determine optimal beam placement without a physician's intervention. The proposed method reduced the dose to OARs, especially for supine treated patients, without any relevant degradation of dose homogeneity and coverage in general. © *2012 American Association of Physicists in Medicine*. [http://dx.doi.org/10.1118/1.3700736]

Key words: breast radiotherapy, automated beam placement, support vector machines

I. INTRODUCTION

Although an effective treatment for breast cancers,[1–3] radiotherapy might cause significant complications in surrounding organs such as the heart and the lung.[4–7] Different treatment positions (e.g., prone vs supine) and treatment techniques [e.g., intensity-modulated radiotherapy (IMRT) with different beam arrangements and (dynamic) wedged tangent fields] have been investigated. However, beam placement is still a manual process that is based on observing anatomical landmarks. It is a subjective procedure, and the result depends on the experience and preference of the physician. The goal of this study is to develop an automated and objective method for determining the optimal tangential beam placement that best separates the organs at risk (OARs) and the region to be treated.

IMRT for whole breast treatment based on direct aperture optimization (DAO) was analyzed and reported[8,9] using either jaws-only or multileaf collimators (MLCs). However, for breast irradiation, tangential beams are generally preferred to minimize dose to OARs.[10] In this paper, we focus on tangential beams defined by jaws-only aperture but also show the ability of the method to optimize lung/heart blocking.

Our approach for optimizing tangential beam placement is a geometrical algorithm. Purdie *et al.*[11] also optimized the tangential beam parameters geometrically; however, their method was basically an exhaustive search, which is less efficient and does not guarantee an absolute minimum of the score function.

Support vector machine (SVM) is a general purpose classification algorithm. It finds a hyperplane in the multidimensional parameter space that separates the whole dataset into two different sets so that the gaps between the hyperplane and the separating sets are as wide as possible. SVM has been widely used for many machine learning and classification problems. In the field of radiation oncology, researchers have used SVM to predict radiotherapy outcomes,[12–14] evaluate volume delineation,[15] for patient positioning,[16] and to judge planning quality.[17]

The nature behind the SVM is similar to our beam placement problem in that we need to find the equation of the optimal separating plane so that the margin between the OARs and the whole ipsilateral breast (WB) is maximized. The separating plane equation found by SVM is then converted into three beam placement parameters: gantry angle, collimator angle, and jaw size. The performance of the SVM-based algorithm on 36 test cases is reported and discussed.

II. METHOD AND MATERIALS

II.A. Problem formulation

Treatment fields are defined by four planes in the three-dimensional (3-D) space. Three of the planes do not play a role in separating the target volumes from the OARs and can be easily set manually; therefore, only the posterior plane between the OARs and the target volumes needs to be optimized. The beam placement problem is therefore equivalent to finding the optimal separating plane between the OARs and the WB with the included clinical target volumes (CTVs).

The OARs include the heart, the ipsilateral lung, and the contralateral breast. The whole breast is defined as the breast volume within a preliminary treatment field placed manually by the physician. This field covers the breast from the clavicular head to 2 cm below the breast, and its posterior plane is aligned with the projections of the midsternum and the anterior aspect of the latissimus dorsi on the skin. Two target volumes are defined: CTV1 is the WB volume minus a 0.5 cm layer adjacent to the skin, and CTV2 encloses the tumor bed with 1.5 cm margin, and excluding regions that extend outside the CTV1. (Naturally, WB encloses CTV1 and CTV1 encloses CTV2.) Our contouring method is described elsewhere.[20,21] The OARs and the target volumes are usually not linearly separable; we therefore need to find a tradeoff between *maximizing* the volume of the WB (and the included CTVs) inside the treatment field and *minimizing* the volume of OARs inside the treatment field. Relative significances are assigned to different volumes (or regions inside thereof). These factors are based on the following clinical constraints and considerations: (1) the treatment field should cover the WB, especially the region that is in close proximity to the tumor; (2) heart sparing is more critical than lung sparing; (3) WB tissue coverage beyond CTV1 can be compromised in exchange for significant dose reduction to the heart and the lung; and (4) dose to the contralateral breast should be avoided.

II.B. Optimal separating plane by support vector machines

Let the surface points of the WB and the included CTVs be labeled $+1$ and the surface points of the OARs be labeled -1, i.e., having a set of 4D vectors $\chi = \{\mathbf{x}_i, y_i\}$, where vector $\mathbf{x}_i$ are the 3D coordinates of the ith point and $y_i = +1$ if $\mathbf{x}_i \in PTV$ (CTVs$\cup$WB) and $y_i = -1$ if $\mathbf{x}_i \in OARs$, for $i = 1...N$. (N is the total number of surface points.) In the simplest form of the SVM formulation,[18] the equation of the optimal separating plane, $g(\mathbf{x}) = \mathbf{w}^T\mathbf{x} + b = 0$ is determined by the solution of the following optimization problem:

$$Minimizing\ \mathbf{w}^T\mathbf{w}, subject\ to\ y_i(\mathbf{w}^T\mathbf{x}_i + b) \geq 1,$$

which maximizes the margin $\frac{2}{\|\mathbf{w}\|}$ between samples with opposite labels.

Usually, the target volumes and the OARs cannot be completely separated by a plane. In this case, positive variables, ξ_i, is introduced as a measure of the violation of the constraints [shown in Fig. 1(b)]. The penalty term $C\sum_{i=1}^{N}\xi_i$ is added to the objective function and new constraints $y_i(\mathbf{w}^T\mathbf{x}_i + b) \geq 1 - \xi_i$ will be applied. Parameter C is the relative significance factor. In general, the value of C can vary from point to point. We used this option only for the WB, in which significance factors were chosen to be inversely proportional to the distance to the closest surface point of the tumor bed. The optimization problem then becomes

$$\min_{\mathbf{w},b,\xi_{ij}} \left\{ \frac{1}{2}\mathbf{w}^T\mathbf{w} + \sum_{i\in\{\text{organs}\}}\sum_{j=1}^{N_i} C_{ij}\xi_{ij} \right\}$$
$$subject\ to\ y_{ij}(\mathbf{w}^T x_{ij} - b) \geq 1 - \xi_{ij}\ i \in \{\text{organs}\},$$
$$j = 1, \ldots, N_i, \quad (1)$$

where N_i is the number of points that belong to organ i, C_{ij} and ξ_{ij} are the significance factor and the constraint violation measure for the jth point of organ i. A larger C_{ij} indicates a larger penalty on misclassification. To solve the optimization problem in Eq. (1), we use LIBLINEAR,[19] an open source library for large-scale linear SVM classification problems.

The significance factors reported in the paper were determined experimentally using CT scans of 10 randomly selected patients. We performed a systematic search in which at each time one significance factor was adjusted while the others kept fixed. There are totally about 30 sets produced and each of them is applied on 10 patients. As multiple dosimetric objectives were used, we searched for sets of weights when improving one objective would deteriorate

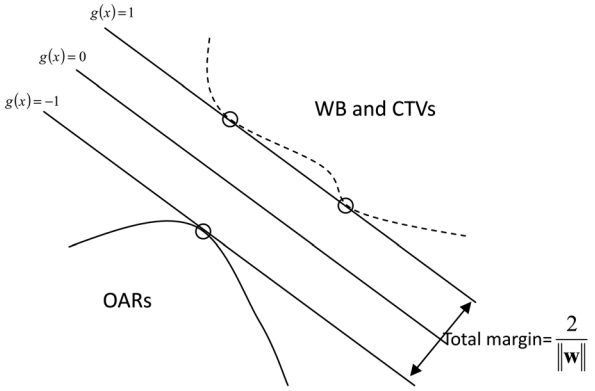

(a) Linearly separable case, where the constraint is $y_i(\mathbf{w}^T\mathbf{x}_i + b) \geq 1$.

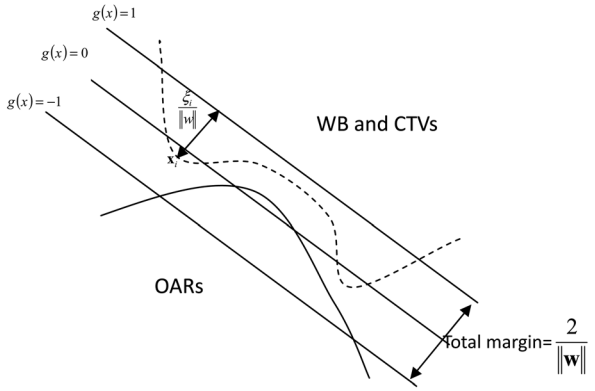

(b) Linearly non-separable case, where the constraint is relaxed by $y_i(\mathbf{w}^T\mathbf{x}_i + b) \geq 1 - \xi_i$.

FIG. 1. Illustration of the support vector machine. Each data point is a three-dimensional vector. Circled points are the support vectors. Solid and dotted lines represent boundaries of OARs and the WB with the included CTVs, respectively.

other(s) (i.e., reached a pareto-optimal point), and then, a subjectively chosen compromise among those points determines the weight factors. For example, the heart/lung significance factor was chosen 3/1. Nevertheless, the user can modify these significance factors. Those determined significance factors were used for all the patients. The derived separating plane is optimal in the maximal margin sense given the selected significance factors C_{ij}.

II.C. Tangential field parameters from the separating plane

Tangential beam placement is controlled by three parameters: gantry angle, collimator angle, and jaw size. Figure 2 illustrates two opposite tangential fields and the associated separating plane. We derived these parameters based on the separating plane determined by the SVM. To be more precise, gantry and collimator angles can be derived by solving the linear equations

$$\mathbf{w} = M_c M_g \mathbf{w}_0, \tag{2}$$

where $\mathbf{w}$ is the normal vector of the optimal separating plane determined by the SVM, $\mathbf{w}_0$ is the normal vector of the plane defined by the X_2—jaw before gantry and collimator rotations, and M_g and M_c are the rotation matrices for the gantry and collimator rotations, respectively. The jaw size is given by the distance from the isocenter to the separating plane.

II.D. Method evaluation

The computed gantry angles, collimator angles, and jaw sizes were compared with those by physicians. Mean,

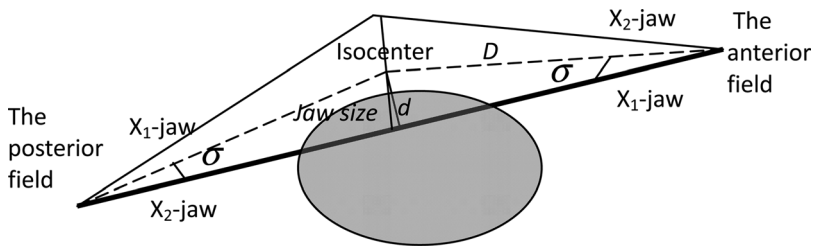

FIG. 2. Two opposite treatment fields in a projection, perpendicular to the Y jaws. The thicker line represents the optimal separating plane determined by the SVM, σ is the angle of the beam divergence, D is the distance between the radiation source and the isocenter, and d is the distance from isocenter to the separating plane.

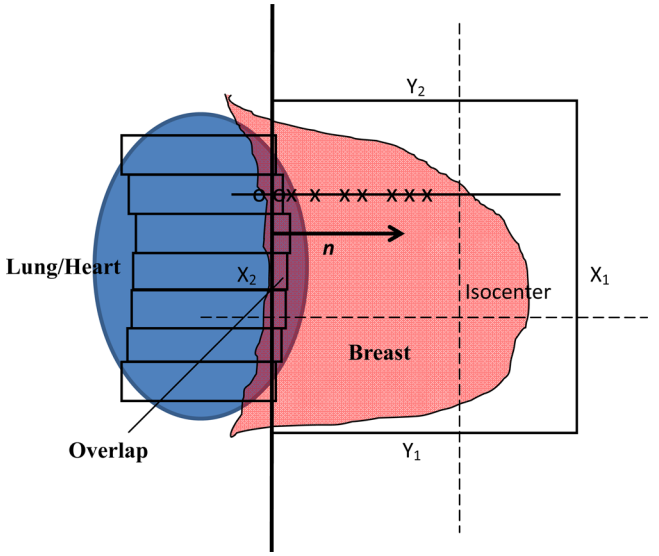

FIG. 3. Treatment field with MLCs from beam eye view. ***n*** is the normal vector of the separating plane, **x** and **o** represent a few projections of the surface points on the breast and avoidance structures respectively within a volume of an MLC leaf path to the midplane of that MLC leaf. These projected points are used in the SVM algorithm to determine that leaf position.

standard deviation, and *p*-value of the differences are computed. The dosimetric measures, including the minimum dose to the CTV2, the maximum dose to CTV2, the V5 (volume at 5 Gy) of the heart, the V10 of the ipsilateral lung, the V95% (volume receiving >95% of the prescribed dose) of the CTV2, and the V95% of the CTV1, were compared with the measures of the treatment plans by physicians. For fair comparison, the minimum CTV2 dose of our method is normalized to the minimum CTV2 dose of the physician's plan. Means and standard deviation of dosimetric measures of manual and automated plans were computed and compared with paired Student t-test.

II.E. Extension of the SVM to block optimization

The technique can be extended to optimize lung/heart blocking by optimizing the posterior field shape. After finding the optimal separating plane based on Sec. II.B., the field is divided into multiple parallel layers (Fig. 3) perpendicular to the posterior field edge. The thickness of the layers was chosen to be 0.5 cm (corresponding 1 MLC leaf thickness in our machines). Surface points within each layer are projected onto the normal vector of the separating plane (which is parallel to the motion of the MLC, if MLC can be used). Determining the posterior edge in one layer is now transformed into a 1-D separation problem, which can be efficiently solved by SVM.

III. RESULTS

We collected treatment/planning data for 23 prone- and 13 supine-treated patients with left breast cancer enrolled in the IRB-approved NYU 05-181 clinical protocol.[16,19,22,23] The actual significance factors C_{ij} in the objective function of the SVM were chosen to be 60 for the heart, 20 for the ipsilateral lung, 120 for the CTV1, 180 for the CTV2, and 60 for the contralateral breast (see Sec. II.B). For the ipsilateral breast, the significance factor for each surface point p_i was set to $\frac{0.1}{d_i}$, where d_i is the distance between p_i and the nearest point on the tumor bed.

The mean and standard deviation in the differences between these parameters for all 36 patients were computed and tabulated in Table I(a). Two-tailed paired T-test showed significant differences in jaw size ($p = 0.0004$) and the gantry angle ($p = 0.039$), and no differences in the collimator angle ($p = 0.90$). Results for the prone- and supine-treated patients are shown separately in Tables I(b) and I(c), respectively. Overall, our proposed method results in smaller jaw size for both groups, significantly for supine-treated patients ($p = 0.0007$ for supine-treated patients but not significant to the 5% level ($p = 0.067$) for prone-treated patients). For supine-treated patients, our method results in smaller jaw size for all of the 13 patients, while only for 14 of the 23 patients in the prone position.

The mean values of five dosimetric measures for all 36 patients were computed and tabulated in Table II(a). Our method reduces the V5 of the heart from 2.7 to 1.7 cm^3, and

TABLE I. Comparison of the gantry angle, collimator angle, and jaw size in the treatment plans between physicians and SVM method: mean and standard deviation of the differences, and *p*-value by paired T-test.

	Mean	Standard deviation	*p*-value
(a) Statistics of beam parameters of all 36 patients (23 prone- and 13 supine-treated)			
Difference between gantry angles (degree)	−0.88	2.4	0.039
Difference between collimator angles (degree)	−0.05	2.2	0.90
Difference between jaw size (mm)	1.4	2.2	0.0004
(b) Statistics of beam parameters of 23 prone-treated patients			
Difference between gantry angles (degree)	−1.03	2.7	0.092
Difference between collimator angles (degree)	0.49	2.4	0.35
Difference between jaw size (mm)	0.87	2.1	0.067
(c) Statistics of beam parameters of 13 supine-treated patients			
Difference between gantry angles (degree)	−0.61	1.7	0.24
Difference between collimator angles (degree)	−1.01	1.6	0.046
Difference between jaw size (mm)	2.4	1.9	0.0007

TABLE II. Comparison of dosimetric measures in the treatment plans by physicians and the SVM method: mean, standard deviation, and *p*-value by paired T-test.

	Manually planned		SVM-based		
	Mean	Std	Mean	Std	*p*-value
(a) Dosimetric statistics of all 36 patients (23 prone- and 13 supine-treated)					
Max dose of CTV2 (%)	108.1	2.0	108.4	2.6	0.55
V5 of heart (cm^3)	2.7	4.8	1.7	2.6	0.058
V10 of Ipsilateral lung (cm^3)	55.2	69.1	40.7	49.4	0.0013
V95% of CTV2 (%)	99.9	0.2	99.9	0.5	0.15
V95% of CTV1 (%)	99.6	0.6	98.8	1.2	0.0002
(b) Dosimetric statistics of 23 prone-treated patients					
Max dose of CTV2 (%)	108.0	2.2	108.3	2.7	0.68
V5 of heart (cm^3)	2.1	2.7	1.7	2.4	0.32
V10 of ipsilateral lung (cm^3)	8.4	14.1	7.3	12.0	0.57
V95% of CTV2 (%)	99.9	0.3	99.8	0.6	0.18
V95% of CTV1 (%)	99.4	0.6	98.7	1.4	0.0087
(c) Dosimetric statistics of 13 supine-treated patients					
Max dose of CTV2 (%)	108.4	1.5	108.6	2.3	0.62
V5 of heart (cm^3)	3.7	7.1	1.7	3.1	0.11
V10 of ipsilateral lung (cm^3)	138.1	45.8	99.9	31.8	0.002
V95% of CTV2 (%)	99.9	0.02	99.9	0.06	0.30
V95% of CTV1 (%)	99.8	0.4	99.1	0.4	0.0007

the V10 of the ipsilateral lung from 55.2 to 40.7 cm^3. The dosimetric measures for prone- and supine-treated patients are shown separately in Tables II(b) and II(c), respectively. For prone-treated patients, the V5 of the heart is reduced from 2.1 to 1.7 cm^3 and the V10 of the ipsilateral lung is reduced from 8.4 to 7.3 cm^3. The differences are not statistically significant. For supine-treated patients, the reductions are from 3.7 to 1.7 cm^3 and from 138.1 to 99.9 cm^3, respectively. The difference for lung is statistically significant ($p = 0.002$). The changes of the V95% of the CTV1 and the CTV2 and the maximum dose to CTV2 are very small in all groups.

For better comparison, the DVHs of the worst and the best case of automatic plan results are shown in Fig. 4. The worst case [Fig. 4(a)] occurred in the prone position. The dose coverage of CTV1 and CTV2 is slightly worse than the manual plan, while the dose for lung is higher (V10 of the lung increased from 13.0 to 39.1 cm^3). The best improvement case [Fig. 4(b)] occurred in the supine position. The V5 of the heart is roughly the same 2.5 cm^3, while the V10 of the ipsilateral lung is reduced from 201.1 to 130.7 cm^3. The V95% of CTV1 is 96.6% compared with 96.1%, while the V95% of CTV2 is the same.

Generally, in the prone position, the difference between manually and computer generated plans were small. For the supine cases, most of automatic plans are preferable to the manual ones because of pronounced dose decreases to heart and lung.

For the blocked fields, the differences with nonblocking tangential fields are generally very small. Table III(a) shows the *average* dosimetric measures for the six patients tested. An example with the largest resulting block shown in Fig. 5, and the corresponding dosimetric measures are in Table III(b). (The MLC in the Fig. 5 is only for illustration; the dose distribution is calculated by using manual blocks of the optimized shape as our machine does not allow MLC blocks and dynamic wedges on the same direction.)

IV. DISCUSSION AND CONCLUSION

The most significant difference between the manual plans determined by physicians and the automated plans determined by our method is the jaw size setting. The plans determined by our method have smaller jaw sizes [see Table I(a)]. The dosimetric comparison between the manual and optimized plans for all patients showed significant improvements in the lung V10 volume, close to significant change in the heart V5 volume, and a very slight but significant decrease of the V95% of the CTV1 (99.6–98.8, $p = 0.002$).

Patients in the supine position seem to benefit more from the proposed method when compared to the prone treated patients. The jaw size is significantly different between the manual and optimized beam placement in both groups, but the difference is larger in the supine than in the prone position. The dosimetric difference of normal tissue is not significant in the prone position, with only a very slight decrease of V95% in the CTV1 (99.4–98.7, $p = 0.009$). For the supine-treated patient, the radiation to lung is largely reduced in the automated beam setup and is both statistically and clinically meaningful. That finding suggests that the prone position even without optimization offers better sparing of the OARs than the supine, in agreement with earlier reports,[9] and the automatic optimization does not improve it much further.

The data indicates that for beam placement in the supine position, the physicians tend to set the beam deeper (2.4 mm, $p = 0.0007$) into the chest wall than necessary. The same

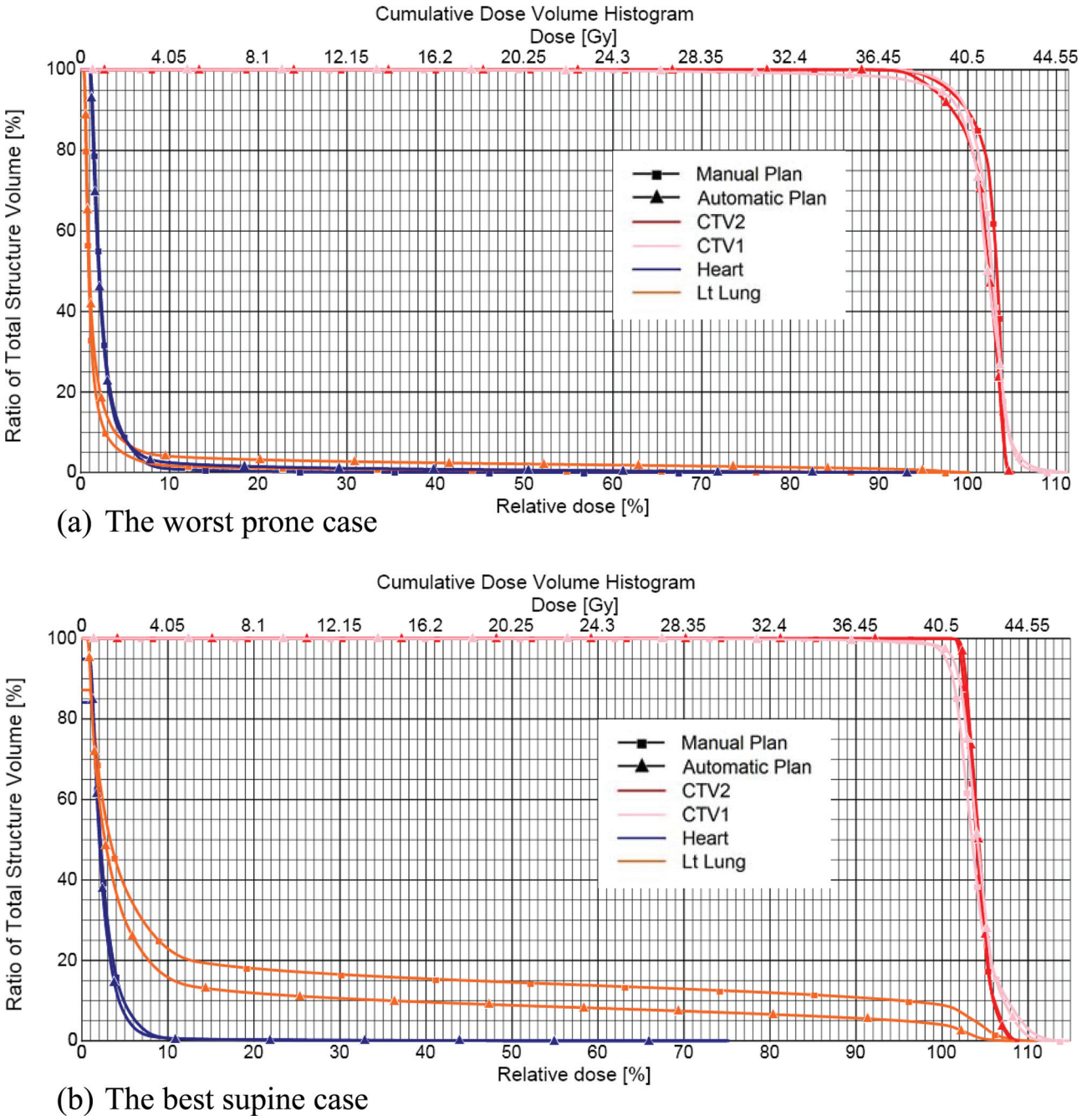

FIG. 4. DVH plot of the worst and best cases of automatic plans (triangle) compared with manual plans (square).

value for the prone position is 0.87 ($p = 0.067$). Also, the underestimated collimator angle ($-1.01°$, $p = 0.046$) could increase the volume of chest wall/lung inside the field. These geometric differences explain the large improvement in the lung V95% volume (138.1–99.9 cm^3, $p = 0.002$) in the supine position between the manual and optimized beam placement. Although the difference of jaw size is small (2.4 mm), the resulting change of dosimetric parameters could be quite large since the distance between the OARs and breast tissue is also very small.

The significance factors adopted in this paper were chosen to reduce the dose to the heart and the lung at the expense of slightly reduced dose homogeneity for the CTVs. By using the same set of significance factors for all patients, our method performed reasonably well. Including more than 10 patients in finding the right significance factors or individualizing the choice using certain anatomical characteristics (e.g., curvature of the chest wall) might result in somewhat different field placements; however, this job can be very challenging and time consuming.

The computation time directly depends on the number of surface points used in the calculation. The computation time for tangential field is within 1 minute for most patients using a computer with a 2.13 GHz Intel i3 dual core processor (Lenovo T410i). Even this short time can be further decreased by using an initial estimate of the separating plane for the

TABLE III. Comparison of dosimetric measures of manual plans, automatic plans with and without MLC blocking.

	Manually planned	w/o blocking	With blocking
(a) Average dosimetric measures of the 6 patients we tested.			
Max dose of CTV2 (%)	109.4	107.6	107.6
V5 of heart (cm^3)	2.05	0.77	0.16
V10 of Ipsilateral lung (cm^3)	59.6	50.2	37.9
V95% of CTV2 (%)	100	99.9	99.7
V95% of CTV1 (%)	99.8	98.2	96.5
(b) Dosimetric measures of the patient shown in Fig. 5.			
Max dose of CTV2 (%)	107.7	104.2	103.3
V5 of heart (cm^3)	4.9	2.1	0
V10 of ipsilateral lung (cm^3)	127.3	124.8	79.5
V95% of CTV2 (%)	100	100	99.4
V95% of CTV1 (%)	100	98.7	94.4

SVM algorithm and by selecting only surface points within a preset distance from the estimated separating plane. However, introducing the lung/heart blocking increases the computation time by a factor of 8–10.

Our decision to focus on unblocked fields in this study stems from practical considerations: In our machines, simultaneous use of dynamic wedge and MLC shaping in the same direction is not possible; therefore, either a physical wedge or a physical block needs to be used. Nevertheless, we demonstrated that our technique can be extended to work with blocks, as the shape of the posterior field border can be determined with the SVM algorithm.

Due to the usually small resulting blocked area, there were only limited dosimetric differences between the blocked and unblocked plans. Table III shows that there is some amount of dose reduction to lung (V10 from 50.2 to 37.9 cm^3 in average), however, at the expense of decreased CTV1 coverage (V95% from 98.2% to 96.5% in average). The limited benefit of blocking might be explained by the fact that the posterior field border and collimator angle is already optimized. Breast and lung (and heart) normally overlap from the beam eye view due to their anatomic geometry. Blocks cannot spare more lung (and heart) without sacrificing breast coverage in this case.

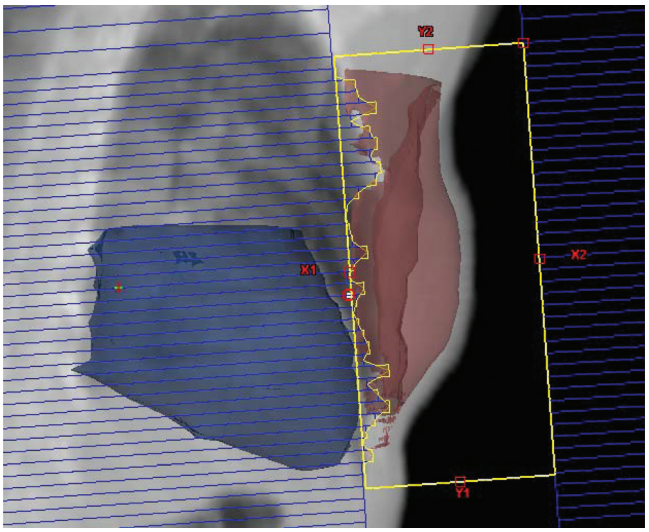

FIG. 5. Treatment field with blocks. The MLCs are illustrated as the blue rectangles and the resulting blocks are in yellow curve.

In conclusion, this study demonstrated the feasibility of using a SVM algorithm to automatically perform optimal beam placement for whole breast radiotherapy in both prone and supine positions. Our SVM-based algorithm used volume-based criteria to find tradeoffs between heart (and lung) volumes that lie within the treatment field and breast volume that lies outside the treatment field. This method is different from other commonly used optimization procedures that are based on dosimetric criteria. The proposed method significantly reduced the dose to the OARs while maintaining acceptable dose homogeneity and coverage over the breast volume to be treated.

ACKNOWLEDGMENTS

Part of this work was presented at the *52nd AAPM Annual Meeting*, July 18–22, 2010, Philadelphia, PA. This work was supported in part by a grant from the Varian Medical System.

[a]Author to whom correspondence should be addressed. Electronic mail: yao@poly.edu; Telephone: (718)-260-3469; Fax: (718)-260-3906.

[1]A. Jemal *et al.*, "Cancer statistics, 2008," Ca-Cancer J. Clin. **58**, 71–96 (2008).
[2]M. Clarke *et al.*, "Effects of radiotherapy and of differences in the extent of surgery for early breast cancer on local recurrence and 15-year survival: an overview of the randomised trials," Lancet **366**, 2087–2106 (2005).
[3]B. Fisher *et al.*, "Twenty-year follow-up of a randomized trial comparing total mastectomy, lumpectomy, and lumpectomy plus irradiation for the treatment of invasive breast cancer," N. Engl. J. Med. **347**, 1233–1241 (2002).
[4]L. B. Marks *et al.*, "The incidence and functional consequences of RT-associated cardiac perfusion defects," Int. J. Radiat. Oncol., Biol., Phys. **63**, 214–223 (2005).
[5]M. Deutsch *et al.*, "The incidence of lung carcinoma after surgery for breast carcinoma with and without postoperative radiotherapy," Cancer **98**, 1362–1368 (2003).
[6]C. W. Hurkmans *et al.*, "Reduction of cardiac and lung complication probabilities after breast irradiation using conformal radiotherapy with or without intensity modulation," Radiother. Oncol. **62**, 163–171 (2002).
[7]L. F. Paszat *et al.*, "Mortality from myocardial infarction following postlumpectomy radiotherapy for breast cancer: a population-based study in Ontario, Canada," Int. J. Radiat. Oncol., Biol., Phys. **43**, 755–762 (1999).
[8]M. A. Earl, M. K. Afghan, C. X. Yu, Z. Jiang, and D. M. Shepard, "Jaws-only IMRT using direct aperture optimization," Med. Phys. **34**(1), 307–314 (2007).
[9]E. E. Ahunbay, G. P. Chen, S. Thatcher, P. A. Jursinic, J. White, K. Albano, and X. A. Li, "Direct aperture optimization-based intensity-modulated radiotherapy for whole breast irradiation," Int. J. Radiat. Oncol. Biol. Phys. **67**(4), 1248–1258 (2007).
[10]G. P. Chen, E. Ahunbay, and X. A. Li, "Automated computer optimization for 3D treatment planning of breast irradiation," Med. Phys. **35**(6), 2253–2258 (2008).
[11]T. G. Purdie, R. E. Dinniwell, D. Letourneau, C. Hill, and M. B. Sharpe, "Automated planning of tangential breast intensity-modulated radiotherapy using heuristic optimization," Int. J. Radiat. Oncol. Biol. Phys. **81**(2), 575–583 (2011).
[12]I. El Naqa, J. D. Bradley, P. E. Lindsay, A. J. Hope, and J. O. Deasy, "Predicting radiotherapy outcomes using statistical learning techniques," Phys. Med. Biol. **54**(18), S9–S30 (2009).
[13]K. Jayasurya, G. Fung, S. Yu, C. Dehing-Oberije, D. De Ruysscher, A. Hope, W. De Neve, Y. Lievens, P. Lambin, and A. L. Dekker, "Comparison of Bayesian network and support vector machine models for

two-year survival prediction in lung cancer patients treated with radiotherapy," Med. Phys. **37**(4), 1401–1407 (2010).
[14]S. Chen, S. Zhou, F. F. Yin, L. B. Marks, and S. K. Das, "Investigation of the support vector machine algorithm to predict lung radiation-induced pneumonitis," Med. Phys. **34**(10), 3808–3814 (2007).
[15]J. Gubbi, A. Kanakatte, K. Tomas, D. Binns, B. Srinivasan, N. Mani, and M. Palaniswami, "Automatic tumor volume delineation in respiratory-gated PET images," J. Med. Imaging Radiat. Oncol. **55**(1), 65–76 (2011).
[16]X. Zhao, E. K. Wong, Y. Wang, S. Lymberis, B. Wen, S. Formenti, and J. Chang, "A support vector machine (SVM) for predicting preferred treatment position in radiotherapy of patients with breast cancer," Med. Phys. **37**(10), 5341–5350 (2010).
[17]X. Zhu, Y. Ge, T. Li, D. Thongphiew, F. F. Yin, and Q. J. Wu, "A planning quality evaluation tool for prostate adaptive IMRT based on machine learning," Med. Phys. **38**(2), 719–726 (2011).
[18]N. Cristianini and J. Shawe-Taylor, *An Introduction to Support Vector Machines and Other Kernel-Based Learning Methods* (Cambridge University Press, Cambridge, England, 2000).
[19]S. Formenti, S. Lymberis, P. Parhar, M. Fenton-Kerimian, C. Magnolfi, B. Wen, J. Chang, and J. DeWyngaert, "Results of NYU 05-181: A prospective trial to determine optimal position (prone versus supine) for breast radiotherapy," Int. J. Radiat. Oncol. Biol. Phys. **75**, S203 (2009).
[20]S. C. Formenti, M. T. Truong, J. D. Goldberg, V. Mukhi, B. Rosenstein, D. Roses, R. Shapiro, A. Guth, and J. K. Dewyngaert, "Prone accelerated partial breast irradiation after breast-conserving surgery: preliminary clinical results and dose-volume histogram analysis," Int. J. Radiat. Oncol. Biol. Phys. **60**(2), 493–504 (2004).
[21]G. Jozsef, J. K. Dewyngaert, S. J. Becker, S. Lymberis, and S. C. Formenti, "Prospective study of cone-beam computed tomography image-guided radiotherapy for prone accelerated partial breast irradiation," Int. J. Radiat. Oncol. Biol. Phys. **81**(2), 568–574 (2011).
[22]S. C. Formenti, D. Gidea-Addeo, J. D. Goldberg, D. F. Roses, A. Guth, B. S. Rosenstein, and K. J. DeWyngaert, "Phase I-II trial of prone accelerated intensity modulated radiation therapy to the breast to optimally spare normal tissue," J. Clin. Oncol. **25**(16), 2236–2242 (2007).
[23]J. Keith DeWyngaert, G. Jozsef, J. Mitchell, B. Rosenstein, and S. C. Formenti, "Accelerated intensity-modulated radiotherapy to breast in prone position: dosimetric results," Int. J. Radiat. Oncol. Biol. Phys. **68**(4), 1251–1259 (2007).